



Xanthine oxidase inhibitors improve energetics and function after infarction in failing mouse hearts

Anna V. Naumova, Vadappuram P. Chacko, Ronald Ouwerkerk, Linda Stull, Eduardo Marbán and Robert G. Weiss

Am J Physiol Heart Circ Physiol 290:837-843, 2006. First published Sep 23, 2005;
doi:10.1152/ajpheart.00831.2005

You might find this additional information useful...

This article cites 49 articles, 27 of which you can access free at:

<http://ajpheart.physiology.org/cgi/content/full/290/2/H837#BIBL>

This article has been cited by 2 other HighWire hosted articles:

Therapeutic Effects of Xanthine Oxidase Inhibitors: Renaissance Half a Century after the Discovery of Allopurinol

P. Pacher, A. Nivorozhkin and C. Szabo
Pharmacol. Rev., March 1, 2006; 58 (1): 87-114.
[\[Abstract\]](#) [\[Full Text\]](#) [\[PDF\]](#)

Xanthine Oxidase Inhibition and Heart Failure: Novel Therapeutic Strategy for Ventricular Dysfunction?

R. J. Hajjar and J. A. Leopold
Circ. Res., February 3, 2006; 98 (2): 169-171.
[\[Full Text\]](#) [\[PDF\]](#)

Updated information and services including high-resolution figures, can be found at:

<http://ajpheart.physiology.org/cgi/content/full/290/2/H837>

Additional material and information about *AJP - Heart and Circulatory Physiology* can be found at:

<http://www.the-aps.org/publications/ajpheart>

This information is current as of September 7, 2006 .

AJP - Heart and Circulatory Physiology publishes original investigations on the physiology of the heart, blood vessels, and lymphatics, including experimental and theoretical studies of cardiovascular function at all levels of organization ranging from the intact animal to the cellular, subcellular, and molecular levels. It is published 12 times a year (monthly) by the American Physiological Society, 9650 Rockville Pike, Bethesda MD 20814-3991. Copyright © 2005 by the American Physiological Society. ISSN: 0363-6135, ESN: 1522-1539. Visit our website at <http://www.the-aps.org/>.



Xanthine oxidase inhibitors improve energetics and function after infarction in failing mouse hearts

Anna V. Naumova,¹ Vadappuram P. Chacko,¹ Ronald Ouwerkerk,¹
Linda Stull,² Eduardo Marbán,³ and Robert G. Weiss³

¹Department of Radiology, Division of Magnetic Resonance Research, and ²Department of Pediatrics, the Johns Hopkins University School of Medicine, Baltimore, Maryland; and ³Department of Medicine, Division of Cardiology, the Johns Hopkins Hospital, Baltimore, Maryland

Submitted 4 August 2005; accepted in final form 6 September 2005

Naumova, Anna V., Vadappuram P. Chacko, Ronald Ouwerkerk, Linda Stull, Eduardo Marbán, and Robert G. Weiss. Xanthine oxidase inhibitors improve energetics and function after infarction in failing mouse hearts. *Am J Physiol Heart Circ Physiol* 290: H837–H843, 2006. First published September 23, 2005; doi:10.1152/ajpheart.00831.2005.—After myocardial infarction, ventricular geometry and function, as well as energy metabolism, change markedly. In nonischemic heart failure, inhibition of xanthine oxidase (XO) improves mechanoenergetic coupling by improving contractile performance relative to a reduced energetic demand. However, the metabolic and contractile effects of XO inhibitors (XOIs) have not been characterized in failing hearts after infarction. After undergoing permanent coronary ligation, mice received a XO inhibitor (allopurinol or oxypurinol) or matching placebo in the daily drinking water. Four weeks later, ¹H MRI and ³¹P magnetic resonance spectroscopy (MRS) were used to quantify *in vivo* functional and metabolic changes in postinfarction remodeled mouse myocardium and the effects of XOIs on that process. End-systolic (ESV) and end-diastolic volumes (EDV) were increased by more than sixfold after infarction, left ventricle (LV) mass doubled ($P < 0.005$), and the LV ejection fraction (EF) decreased ($14 \pm 9\%$) compared with control hearts ($59 \pm 8\%$, $P < 0.005$) at 1 mo. The myocardial phosphocreatine (PCr)-to-ATP ratio (PCr/ATP) was also significantly decreased in infarct remodeled hearts (1.4 ± 0.6) compared with control animals (2.1 ± 0.5 , $P < 0.02$), in agreement with prior studies in larger animals. The XOIs allopurinol and oxypurinol did not change LV mass but limited the increase in ESV and EDV of infarct hearts by 50%, increased EF ($23 \pm 9\%$, $P = 0.01$), and normalized cardiac PCr/ATP (2.0 ± 0.5 , $P < 0.04$). We conclude that XOIs improve ventricular function after infarction and normalize high-energy phosphate ratio in heart failure. Thus XO inhibitor therapy offers a new and potentially complementary approach to limit the adverse contractile and metabolic consequences after infarction.

postinfarction remodeled myocardium; cardiac metabolism; magnetic resonance spectroscopy; allopurinol

VENTRICULAR REMODELING OCCURS after myocardial infarction (MI) in many species, including humans, and is typically characterized by progressive ventricular dilatation, eccentric hypertrophy, and contractile dysfunction (27, 36, 38). Patients with post-MI remodeling experience increased rates of heart failure and cardiovascular mortality, whereas interventions that reduce geometric ventricular remodeling improve outcomes (27, 40, 41, 44). In addition to the geometric and contractile abnormalities associated with post-MI remodeling, adverse changes in energy metabolism also occur (15, 29, 32).

Abnormalities in energy metabolism after MI include reductions in ATP, phosphocreatine (PCr), and in the activity of the creatine kinase (CK) reaction, the primary energy reserve reaction of the heart (20, 21, 29, 31). Inhibitors of CK significantly increase mortality after experimental infarction (16). The reduction in cardiac PCr-to-ATP ratio (PCr/ATP) in experimental postinfarction remodeling is similar to that observed in human heart failure, which, in turn, correlates with clinical severity and predicts overall and cardiovascular mortality (4, 10, 15, 31, 34, 49). Taken together, the energetic consequences of post-MI remodeling are similar to those of heart failure and offer an additional potential mechanism that may contribute to progressive dysfunction and geometric changes.

Xanthine oxidase (XO) is important in purine metabolism, and its expression and activity are increased in heart failure (1). XO is also a major source of free radicals, such as superoxide, that can impair energy metabolism and reduce energetic efficiency (7, 11). In nonischemic experimental and human heart failure, inhibition of XO improves mechanoenergetic coupling by improving contractile performance relative to a reduced energetic demand (7, 11). Targeted XO blockade impacts on the progression of postischemic cardiomyopathy in mice (43) and attenuates left ventricular (LV) remodeling processes after experimental MI (12). Despite the evidence for improved mechanoenergetic coupling with XO inhibition in nonischemic heart failure, the metabolic and contractile effects of XO inhibition on postinfarction remodeling and the effects of XO inhibitors (XOIs) on depressed energetics in failing hearts have not been characterized.

There were two aims to this study. The first aim was to determine the extent to which geometric, contractile, and metabolic remodeling occur *in vivo* after nonreperfused MI in the mouse. The second aim was to test the hypothesis that XOIs improve bioenergetics and contractile function in the failing heart. This is based on the mechanism observed in nonischemic heart failure where XOIs improve mechanoenergetic coupling by improving contractile performance relative to a reduced energetic demand, such that improved energetics, as indexed by the cardiac PCr/ATP, would be expected to be associated with improved contractile function.

MATERIALS AND METHODS

All procedures and protocols were reviewed and approved by the Institutional Animal Care and Use Committee of the Johns Hopkins University.

Address for reprint requests and other correspondence: R. G. Weiss, Carnegie 584, The Johns Hopkins Hospital, 600 N. Wolfe St., Baltimore, MD 21287-6568 (e-mail: rweiss@jhmi.edu).

The costs of publication of this article were defrayed in part by the payment of page charges. The article must therefore be hereby marked "advertisement" in accordance with 18 U.S.C. Section 1734 solely to indicate this fact.



MI in mice. Anesthesia was induced in adult mice (20–30 g) by inhalation of methoxyflurane and maintained with intraperitoneal injection of etomidate (20 mg/kg) and with subcutaneous buprenorphine (0.24 mg/kg). Additional doses of etomidate were administered as needed. Mice were intubated and ventilated with a custom-made ventilator, and the body temperature was maintained constant as monitored with a rectal probe. A left thoracotomy and pericardiectomy were performed, and the left main coronary artery was completely ligated with suture. After verification that coronary occlusion had occurred by blanching of the tissue distal to the suture, the ribs were closed with suture and the mice recovered. Additional doses of buprenorphine (0.96 mg/kg) were administered to limit discomfort. Immediately after MI surgery, XO-inhibited mice received either allopurinol (0.5 mM) or oxypurinol (1 mM) in the drinking water, whereas control animals had neither. These concentrations were previously shown to inhibit XO in this model (43). Because few pharmacological agents are completely specific, we studied both allopurinol and oxypurinol to increase the likelihood that any observed metabolic or contractile effects were due to XO inhibition and not due to another effect of one agent. All animals underwent MRI and magnetic resonance (MR) spectroscopy (MRS) studies 4 wk after surgery.

MRI and MRS. Experiments were performed by using a General Electric Omega NMR spectrometer and Bruker Medical BioSpec Spectrometer (Bruker BioSpin) equipped with a 4.7 T/40 cm Oxford magnet and a 15 cm (ID) actively shielded Accustar gradient set (8, 47).

Mice were anesthetized with 1% isoflurane in oxygen (1 l/min) delivered through a nose cone and placed in a custom-constructed ¹H coil with the heart centered over the ³¹P coil (8, 47) on a flat Plexiglas platform with temperature control (37 ± 1°C). The mice were rotated to the left so that the uninvolved septum was centered over the surface coil, thus minimizing contributions from the infarcted lateral wall. Single-lead ECG was recorded from platinum electrodes attached to each animal's extremities and was used to trigger the MRI acquisitions using commercial software (Small Animal Monitoring and Gating System SA Instrument, Stony Brook, NY).

High-resolution, spin-echo transverse ¹H MR images (echo time, 11 ms; recycle time, 500 ms; slice thickness, 2 mm; field of view, 32 mm; and acquisition time, 2 min) were obtained to define the regions of metabolic interest, as well as to confirm the position of the LV over the center of the ³¹P MRS surface coil (11 mm, OD), and to quantify LV function. A set of multi-slice short-axis images (slice thickness, 1.2 mm without gap between slices) for end systole and another for end diastole were acquired. Each slice was acquired exactly at the same time during R-R interval in cardiac cycle. Epicardial and endocardial borders were manually delineated for determination of LV volumes at end systole and end diastole (ESV and EDV, respectively) and LV mass using the software package National Institutes of Health (NIH) Image version 1.52 (Bethesda, MD) for a Macintosh computer. Total LV volumes were calculated as the sum of all slice volumes. Stroke volume (SV) was calculated as EDV minus ESV and cardiac output as SV multiplied by heart rate. The LV ejection fraction (EF) was calculated from the relative difference in EDV and ESV.

Myocardial infarct size was determined from short-axis systolic images. The circumference of the LV that was thinned due to infarction (systolic wall thickness <0.5 mm) was compared with that of viable tissue, and a score was assigned as a percentage of overall ventricular circumference (14). For each heart, the mean score was determined from all of the image slices.

Spatially localized ³¹P MR spectra were acquired after optimization of the magnetic field homogeneity using the ¹H coil to shim on a thick slice containing the heart. A one-dimensional chemical shift imaging sequence was used with 32 phase-encode steps in the direction perpendicular to the plane of the coil. The time of the phase-encode gradient was 0.5 ms, the field of view 32 mm, the recycle delay 1 s, and 64 averages were obtained per phase-encode step.

Adiabatic pulses with a flip angle of 45° were used for uniform excitation. Total acquisition time was ~34 min. With this protocol, well-resolved spectra from 1-mm slices from the antero-septal region of the mouse heart parallel to the coil were obtained (8, 47). In a prior study (47) these noninvasive image-guided ³¹P MRS techniques gave identical results to those obtained from invasive measures, indicating minimal contamination from surrounding structures with this approach (47). All mice awoke within ~1 min after completing the MRI/MRS examination.

³¹P spectra were analyzed with a combination of custom (3) and proprietary (NIH Image, Bethesda, MD) software. The PCr/ATP was determined from the integrated peak areas of the PCr and [β-P]ATP resonances from voxels centered on skeletal muscle in the anterior chest or on cardiac muscle identified from the high-resolution ¹H MR images, as described previously (8). Voxel shifting was performed when necessary to optimize slice alignment with cardiac structures and to minimize skeletal muscle contamination of cardiac spectra (5). The PCr/ATP values were corrected for partial saturation effects using a factor determined in separate studies (6, 8, 46, 47) that included fully relaxed acquisitions. Infarcted, nonviable myocardium lacks PCr and ATP (45, 48). In prior ³¹P MRS studies (16, 18, 19, 32, 33, 37) of infarcted rodent hearts, the detected PCr and ATP signals were attributed to the surviving viable regions, even when the entire infarcted region was contained within the region studied by MRS. Based on this accepted practice and our efforts through animal positioning and slice selection to minimize infarcted tissue within the volume of interest, the cardiac PCr/ATP values reported here derive almost entirely from surviving, viable myocardium. Data were compared by ANOVA with STATISTICA software (StatSoft, Tulsa, OK). Differences were considered statistically significant at *P* < 0.05. All data means ± SD.

RESULTS

Postinfarction remodeling in mice. The mean body weight for all animals was 29 ± 2 g, and there were no statistically significant differences among the groups. There were no significant anatomic, functional, or metabolic differences between allopurinol- and oxypurinol-treated hearts, so the groups were combined (MI+XOI) (Table 1).

Representative ¹H MR cardiac images acquired at end systole and end diastole are shown in Fig. 1 for a normal mouse (control) and in another after MI. Four weeks after MI, there was a significant increase in mean LV mass, a severalfold increase in LV chamber dimensions, and a significant reduction in EF, as shown in Table 1. Specifically, LV end-diastolic and end-systolic dimensions were increased by more than sixfold, and mean LV ejection fraction decreased from ~60% to 15% (Table 1). After infarction, LV mass doubled (*P* < 0.001) and the ratio of myocardial mass-to-chamber volume was reduced severalfold (*P* < 0.001, Table 1), consistent with prior observations (36, 38) in infarct-remodeled hearts. Together, these findings in MI mice demonstrate a marked degree of geometric remodeling and LV dysfunction that occurs in this model of permanent left main coronary artery occlusion.

To determine whether myocardium remote from infarction demonstrates energetic abnormalities in the mouse similar to those observed in larger animals, we used noninvasive image-guided ³¹P MRS to quantify cardiac high-energy phosphates. Representative *in vivo* cardiac ³¹P MR spectra from normal and infarct animals are shown in Fig. 2. In control mice, the mean PCr/ATP is 3.0 ± 0.6 in chest skeletal muscle and 2.1 ± 0.5 in heart. These agree well with previously published values in mice (8, 47), as well as those in larger species, including

Table 1. ^1H MR imaging results

Group	n	ESV, mm ³	EDV, mm ³	SV, mm ³	CO, mm ³ /min	LV mass, mg	LV mass/ESV, mg/mm ³	LV mass/EDV, mg/mm ³	MI size, %	EF, %
Normal control mice without MI	9	13±5	31±7	18±2	8,900±1,500	80±11	6.8±2.2	2.6±0.4		59±8
MI group, 4 wk after surgery	11	182±129*	203±133*	21±9	9,600±4,700	162±29*	1.4±0.9*	1.2±0.7*	55±11	14±9*
MI mice + allopurinol, 0.5 mM	7	84±29*	108±36*	23±11	10,500±49,000	139±16*	1.8±0.6*	1.4±0.5*	48±8	21±7*†
MI mice + oxypurinol, 1 mM	11	104±66*	131±75*	28±14	13,200±7,300	159±32*	2.0±0.9*	1.4±0.9*	50±9	24±10*‡
XOIs, allopurinol and oxypurinol combined	18	96±54*‡	122±62*‡	26±13	12,200±6,400	151±28*	1.9±0.8*	1.4±0.5*	49±9	23±9*§

Values are means ± SD; n = number of mice. MR, magnetic resonance; ESV, end-systolic volume; EDV, end-diastolic volume; SV, stroke volume; CO, cardiac output; LV, left ventricular; MI, myocardial infarction; EF, ejection fraction; XOIs, xanthine oxidase inhibitors. * $P < 0.005$ vs. normal control mice; † $P < 0.08$ vs. MI group; ‡ $P < 0.03$ vs. MI group; § $P < 0.01$ vs. MI group.

humans (6, 26, 46). In contrast, infarct remodeled myocardium is characterized by a significant 30% decrease in the mean cardiac PCr/ATP to 1.4 ± 0.6 ($P < 0.02$).

Effects of XOIs in remodeled mouse myocardium. XO therapy did not affect the increase in LV mass that develops after infarction but did significantly attenuate the marked degree of ventricular dilatation that occurs (Table 1). Specifically, XOIs attenuated the dramatic increase in ESV ($P = 0.02$) and EDV ($P = 0.03$) after infarction (Table 1). In addition, LV EF was significantly higher in all MI+XOI hearts ($23 \pm 9\%$) than in MI hearts ($14 \pm 9\%$, $P = 0.01$). Infarct size did not significantly differ between control and XO hearts ($55 \pm 11\%$ and $49 \pm 9\%$, respectively; $P = 0.10$, Table 1), in accord with prior histopathological findings in this model (43).

XO inhibition with allopurinol and oxypurinol after infarction normalized myocardial PCr/ATP (Fig. 3). The mean myocardial PCr-to-ATP ratios were 2.1 ± 0.7 and 1.9 ± 0.4 for allopurinol and oxypurinol, respectively. The cardiac PCr/ATP was significantly higher in MI+XOI (2.0 ± 0.5) than in MI mice (1.4 ± 0.6 , $P < 0.04$) and similar to that in normal, noninfarcted mice.

There was a correlation between the metabolic and functional parameters in MI and MI+XOI hearts (Fig. 4) in that the correlation coefficient between PCr/ATP and ESV was -0.7 ($P < 0.05$) and between PCr/ATP and EF, $r = 0.65$ ($P < 0.05$). Thus XO inhibition normalizes the reduced cardiac PCr/ATP in these failing, infarct-remodeled mouse hearts, and this is associated with improved contractile function.

DISCUSSION

The geometric, functional, and energetic consequences of post-MI remodeling were noninvasively characterized in a murine model of heart failure as well as the effects of XOIs on that process. We conclude that significant ventricular geometric remodeling occurs 4 wk after permanent coronary ligation in the mouse as evidenced by a doubling in LV mass, severalfold increases in EDV and ESV, as well as a marked reduction in LV EF (Table 1). The magnitude of these changes is comparable or larger than observed in other species (36). Less dramatic changes in mass, chamber dimensions, and EF have been reported in mice after reperused infarction (50) and

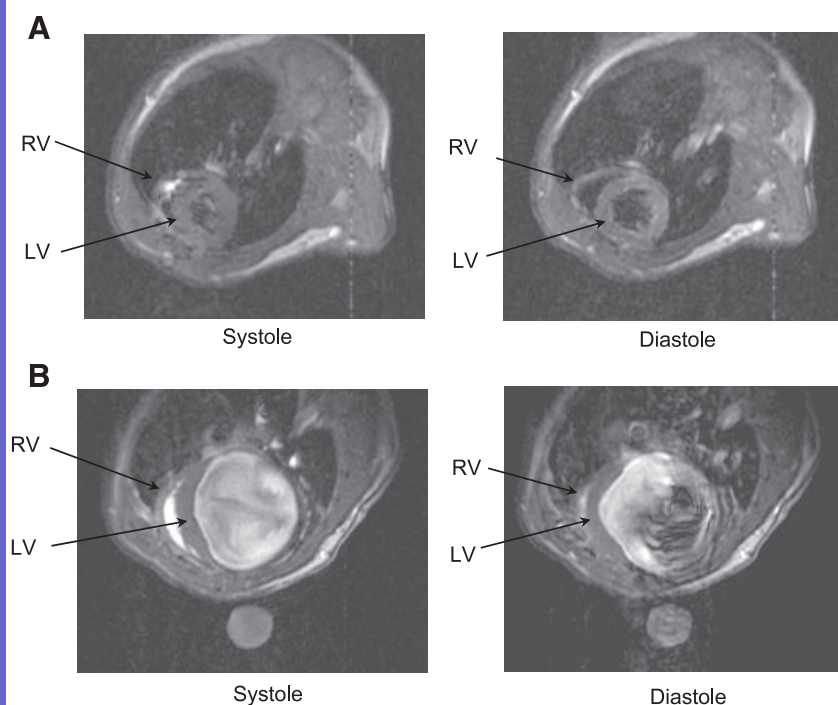


Fig. 1. Typical transverse short-axis ^1H magnetic resonance (MR) images of mouse thorax at level of heart at end systole (A and B, left) and end diastole (A and B, right) for normal mouse (control, A) and another 4 wk after MI (B). After infarction there is severalfold increase in left ventricular (LV) dimensions and relative decrease in amount of blood ejected. As a side note, blood in ventricular chamber appears dark in normal mouse because blood with excited spins has exited chamber during time of spin-echo sequence. In contrast, blood in ventricular chamber remains bright in postmyocardial infarction (post-MI) heart with same spin-echo sequence because only small fraction of chamber blood with excited spins has exited chamber. RV, right ventricle.

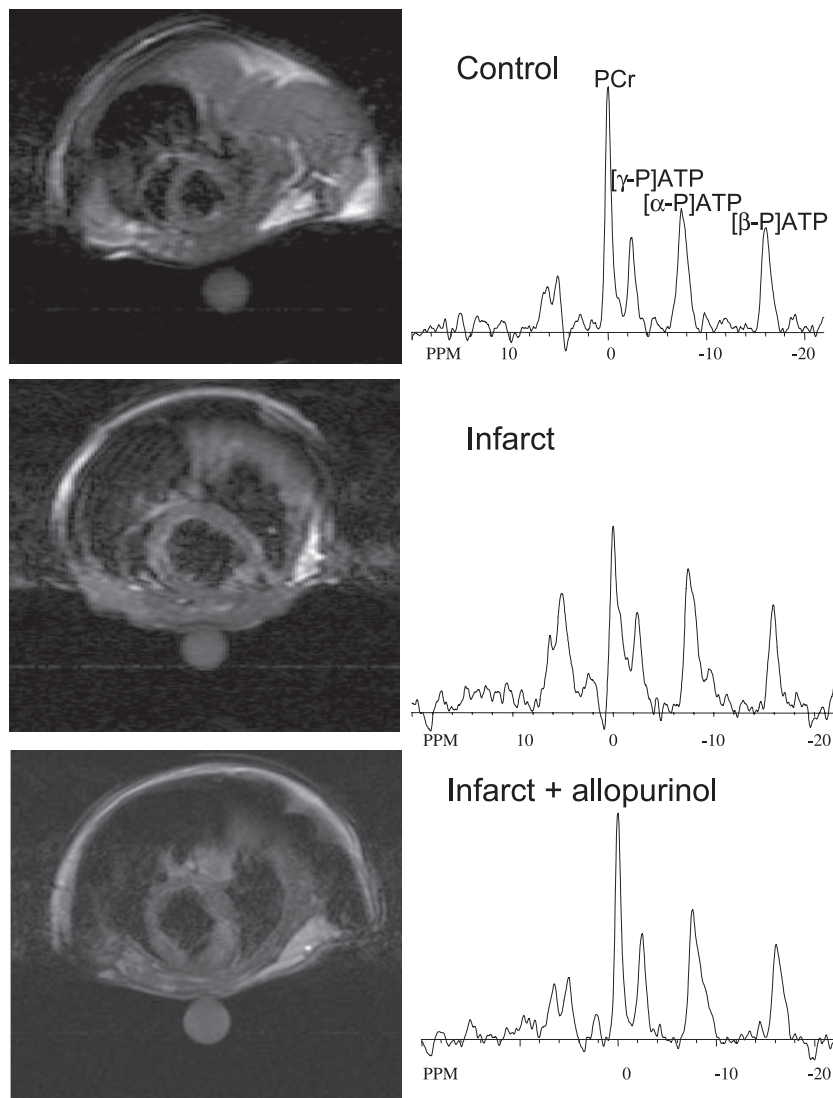


Fig. 2. MR images (*left*) and ³¹P spectra (*right*) in normal (*right, top*), infarct-remodeled (*right, middle*), and infarct-remodeled with xanthine oxidase (XO) inhibitor (XOI) allopurinol (*right, bottom*) mouse hearts. ³¹P MR spectra with 1-dimensional chemical shift imaging were nominally obtained from 1-mm slices from antero-septal region of mouse heart parallel to coil (*left*). Cardiac phosphocreatine (PCr)-to-ATP ratio (PCr/ATP) is reduced in failing myocardium and normalized with chronic allopurinol administration. PPM, parts per million.

earlier than 4 wk after permanent coronary ligation (13). Less remodeling was also observed in other studies (30) where smaller infarct sizes ($18 \pm 2\%$) were induced than in this study (~50%), likely due to more proximal coronary ligation in our approach. The decrease in the ratio of LV mass to chamber volume is similar to that reported in other models with large infarctions after coronary occlusion (36, 38).

In addition, we observed a significant 30% reduction in the *in vivo* myocardial PCr/ATP in infarcted hearts. These data demonstrate that metabolic remodeling, at least in relation to the CK reaction, occurs *in vivo* in the postinfarction, failing mouse, and they are in agreement with prior observations (23, 29, 49) in patients and in larger animals after infarction. Taken together, they demonstrate that remodeling occurs in the mouse and suggest that transgenic murine lines may offer novel avenues for investigating additional mechanisms underlying postinfarction anatomic and energetic remodeling.

Marbán's laboratory (43) recently showed that XO activity is increased in this mouse infarction model and that oral allopurinol suppresses this increase and improves both *in vitro* and *in vivo* contractile function as well as survival. The current MRI findings in different animals confirm the prior observation

made with echocardiography that XO inhibition improves *in vivo* contractile function after infarction in the mouse and does so without preventing hypertrophy. In the earlier work, the improved contractile function with XOI was not associated with increased activator calcium or a left shift in calcium sensitivity but rather was due to an increase in force production during maximal calcium activation (43). Because allopurinol restored myofilament force generation to near-normal values without altering intracellular $[Ca^{2+}]_i$, the hypothesis was generated that XO inhibition improves the poor coupling between energy production and mechanics in failing hearts. Simply put, the ability to generate more force without augmenting activator calcium predicts an improved efficiency of myocardial energy utilization.

Energy metabolism fuels normal myocardial contractile function, and for decades it has been hypothesized that a deficit in energy metabolism may contribute to the contractile deficit in heart failure (21, 22). Likewise, a deficit in energy metabolism could contribute to the progressive dysfunction and geometric changes after infarction (29). The CK reaction reversibly converts the major cardiac form of chemical energy ATP with the prime energy reserve metab-

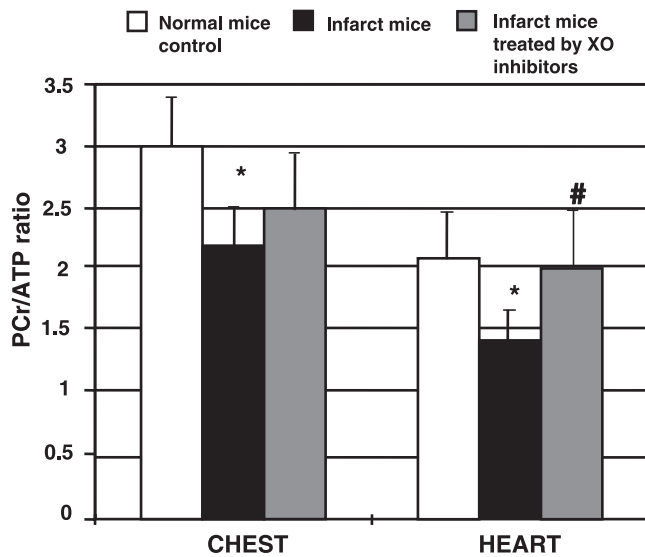


Fig. 3. In vivo PCr/ATP values in chest muscle (left) and cardiac muscle (right) from control (white bars, $n = 10$), MI (black bars, $n = 9$), MI+XOIs (gray bars, $n = 10$) mice. * $P < 0.02$, statistically significant difference with control group (normal mice); # $P < 0.02$, statistically significant difference with MI group.

olite PCr. Animal models of heart failure and patients with heart failure typically exhibit abnormalities in the CK reactants with modest reductions in [ATP], larger reductions in [PCr] and total creatine, and significant reductions in the cardiac PCr/ATP (4, 10, 15, 16, 29, 34). Abnormalities, such as a reduced PCr/ATP, correlate with the severity of the heart failure, improve with clinical recovery, and are stronger predictors of mortality than usual clinical indexes of LV EF and the New York Heart Association class (31). All of these observations are consistent with but do not prove that the abnormalities in energy metabolism may contribute to the pathophysiology of the contractile dysfunction in heart failure. To test the energy starvation hypothesis of heart failure, one needs to determine whether a metabolic intervention that improves energetics results in improved contractile function in failing hearts. Evidence that overexpression of a glucose transporter in pressure-overload mice attenuates the development of heart failure (24) and that ranolazine, a free fatty-acid inhibitor, improves mechanical efficiency in dogs with heart failure (9) both indicate that metabolic interventions can be important in heart failure. However, here the energetic changes may be secondary to improved excitation-contraction coupling, rather than reflecting a primary metabolic effect.

In this regard, the current studies on XO inhibition in remodeled mouse myocardium provide important insights. XO inhibition improves mechanoenergetic coupling in failing hearts by reducing energetic demand in both animals and people (7, 11). Improved mechanoenergetic efficiency with XO inhibition occurs in failing but not normal hearts and is due to a reduction in myocardial oxygen consumption while maintaining or improving contractile function. Thus XO inhibition represents one strategy for evaluating the energy starvation hypothesis of heart failure.

We report here that XO inhibition normalizes the reduced myocardial PCr/ATP in failing mouse hearts. The improve-

ment in cardiac PCr/ATP with XO is not likely due to an effect on infarct size because it is similar in control and infarcted hearts (Ref. 43, and see RESULTS) and because infarcted tissue does not contain significant PCr or ATP (45, 48). XO is one of the first metabolic interventions that normalize reduced cardiac energetics in any model of heart failure. Moreover, improved energetics with XO inhibitors are associated with improved contractile function (EF, Table 1). Although angiotensin-converting enzyme (ACE) inhibition prevents the decrease of in vitro CK activity in infarcted rat hearts (17), ACE inhibition has many effects including those on LV hypertrophy and cardiac demand that can secondarily affect metabolism. Thus XO inhibition represents a metabolic approach to improve altered energetics after infarction in a failing heart, and this is associated with a significant improvement in contractile function in that setting.

Why is the cardiac PCr/ATP lower in remodeled failing myocardium, and what is the mechanism by which XO inhibition improves it? Myocardial PCr/ATP falls acutely during

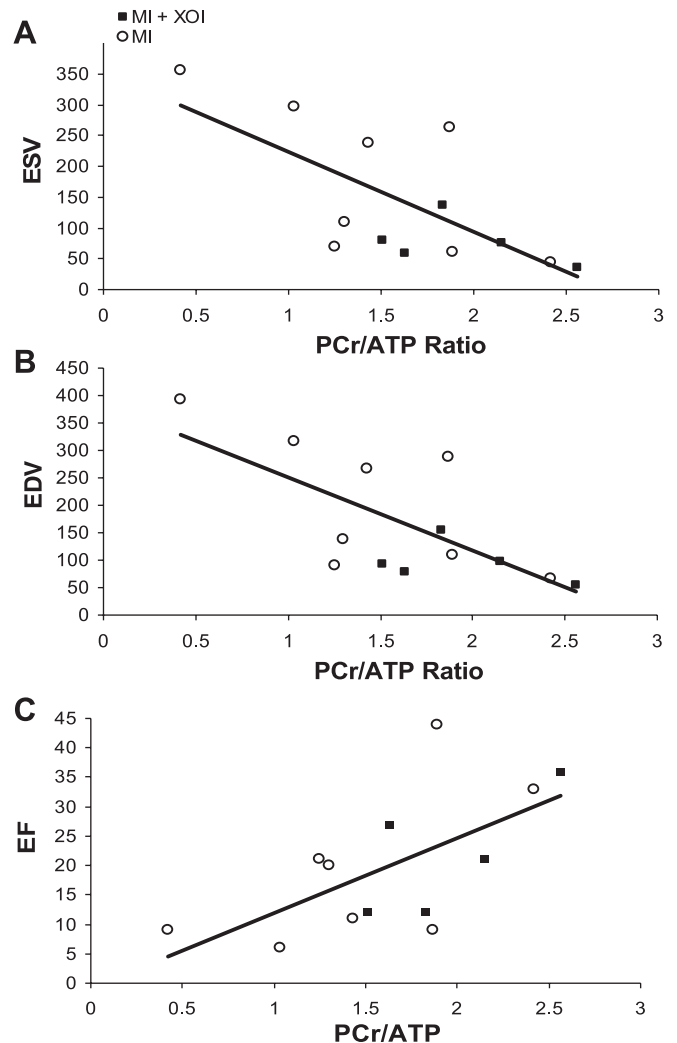


Fig. 4. Relationship between end-systolic volume [ESV, A, where $ESV = -130.63 (PCr/ATP) + 354.64$; $r = -0.7$], end-diastolic volume [EDV, B, where $EDV = -133.76 (PCr/ATP) + 384.2$; $r = -0.7$], and ejection fraction [EF, C, where $EF = 12.761 (PCr/ATP) - 0.821$; $r = 0.65$] and myocardial PCr/ATP in MI (○) and MI+XOI (■) hearts.



ischemia as a result of an imbalance of oxygen supply and demand whereby PCr is consumed to buffer or delay a decline in ATP. In the more chronic setting of heart failure, there is evidence that classic ischemia is not present in that deoxy-myoglobin cannot be detected in several animal models of heart failure (2, 28). However, a slow loss in ATP does occur in heart failure that is accompanied by a more rapid and greater loss of total creatine (42). Creatine depletion acts to attenuate or prevent an increase in ADP as ATP falls (42). Because creatine is not synthesized in muscle cells, if expression of the major creatine transport proteins in animal models and patients with heart failure is depressed (35), then this may be the likely mechanism for the decrease in total creatine in heart failure. It seems likely that by improving mechanoenergetic coupling in dysfunctional myocardium and/or blocking adenine nucleotide degradation, XO inhibition attenuates the initial ATP loss and the resultant more dramatic decline in PCr/ATP. An alternative explanation posits that XOIs fundamentally alter cross bridge kinetics, such that more force is generated per ATP consumed. Such a mechanism has been proposed to underlie the effects of agents, such as XOIs, that increase maximal calcium-activated force without shifting the calcium-force relationship (39). We cannot exclude the possibility that XO inhibition exerts an antioxidant protective effect in the heart. The present data do not distinguish among these various mechanisms, which merit further dissection.

In conclusion, geometric, functional, and metabolic remodeling occurs in this mouse postinfarction model, and the magnitude of the changes is similar or greater than those observed in other larger mammals. XO inhibition attenuates but does not prevent the geometric changes, significantly improves contractile function, and completely normalizes depressed cardiac high-energy phosphate ratios. Because XO inhibition improves depressed energetics in postinfarction heart failure, additional studies of XO inhibition in other models of heart failure are warranted. The observation that a metabolic intervention normalizes energetics and results in improved contractile function directly supports the long-debated energy starvation hypothesis of heart failure. The widespread clinical availability of XO inhibitors should speed clinical trials of the metabolic and functional effects of XO inhibition in human heart failure. Those trials would ultimately determine whether XO inhibition represents an additional therapeutic option to complement ACE inhibitors, β -blockers, and aldosterone inhibitors after infarction.

ACKNOWLEDGMENTS

We thank Michelle Leppo for performing MI surgery on the mice. Present address: A. Naumova: University of Washington, 815 Mercer St., Office 131A, Seattle, WA 98109; Present name and address of L. Stull: Linda Marbán, Excigen, Inc., 2415 Old Bosley Rd., Lutherville, MD 21093.

GRANTS

This work was supported by National Heart, Lung, and Blood Institute Grant HL-63030 (to R. G. Weiss) and R01-HL-44065 (to E. Marbán).

DISCLOSURES

E. Marbán holds the Michel Mirowski, MD Professorship of Cardiology of the Johns Hopkins University. Under a licensing agreement between Cardiome Pharma Corporation and the Johns Hopkins University, E. Marbán is entitled to a share of royalty received by the University on sales of products described in this article. E. Marbán and the University own Cardiome Pharma Corporation stock, which is subject to certain restrictions under University policy. E.

Marbán is a paid member of the Cardiome Pharma Corporation Scientific Advisory Board. The terms of this arrangement are being managed by the Johns Hopkins University in accordance with its conflict of interest policies.

REFERENCES

1. Abadeh S, Case PC, and Harrison R. Purification of xanthine oxidase from human heart. *Biochem Soc Trans* 21: 99S, 1993.
2. Bache RJ, Zhang J, Murakami Y, Zhang Y, Cho YK, Merkle H, Gong G, From AH, and Ugurbil K. Myocardial oxygenation at high workstates in hearts with left ventricular hypertrophy. *Cardiovasc Res* 42: 616–626, 1999.
3. Barker PB and Sibisi S. Non-linear least squares analysis of in vivo ³¹P NMR data (Abstract). *Soc Magn Res Med* 9: 1089, 1990.
4. Beer M, Seyfarth T, Sandstedt J, Landschutz W, Lipke C, Kostler H, von Kienlin M, Harre K, Hahn D, and Neubauer S. Absolute concentrations of high-energy phosphate metabolites in normal, hypertrophied, and failing human myocardium measured noninvasively with ³¹P SLOOP magnetic resonance spectroscopy. *J Am Coll Cardiol* 40: 1267–1274, 2002.
5. Bottomley PA, Hardy CJ, Roemer PB, and Weiss RG. Problems and expediencies in human ³¹P spectroscopy. The definition of localized volumes, dealing with saturation and the technique-dependence of quantification. *NMR Biomed* 2: 284–289, 1989.
6. Bottomley PA, Hardy CJ, and Weiss RG. Correcting human heart ³¹P NMR spectra for partial saturation. Evidence that saturation factors for PCr/ATP are homogeneous in normal and diseased states. *J Magn Reson* 95: 341–355, 1991.
7. Cappola TP, Kass DA, Nelson GS, Berger RD, Rosas GO, Kobeissi ZA, Marbán E, and Hare JM. Allopurinol improves myocardial efficiency in patients with idiopathic dilated cardiomyopathy. *Circulation* 104: 2407–2411, 2001.
8. Chacko VP, Aresta F, Chacko SM, and Weiss RG. MRI/MRS assessment of in vivo murine cardiac metabolism, morphology, and function at physiological heart rates. *Am J Physiol Heart Circ Physiol* 279: H2218–H2224, 2000.
9. Chandler MP, Stanley WC, Morita H, Suzuki G, Roth BA, Blackburn B, Wolff A, and Sabbah HN. Short-term treatment with ranolazine improves mechanical efficiency in dogs with chronic heart failure. *Circ Res* 91: 278–280, 2002.
10. Conway MA, Allis J, Ouwerkerk R, Niioka T, Rajagopalan B, and Radda GK. Detection of low phosphocreatine to ATP ratio in failing hypertrophied human myocardium by ³¹P magnetic resonance spectroscopy. *Lancet* 338: 973–976, 1991.
11. Ekelund UE, Harrison RW, Shokek O, Thakkar RN, Tunin RS, Senzaki H, Kass DA, Marbán E, and Hare JM. Intravenous allopurinol decreases myocardial oxygen consumption and increases mechanical efficiency in dogs with pacing-induced heart failure. *Circ Res* 85: 437–445, 1999.
12. Engberding N, Spiekermann S, Schaefer A, Heineke A, Wiencke A, Muller M, Fuchs M, Hilfiker-Kleiner D, Hornig B, Drexler H, and Landmesser U. Allopurinol attenuates left ventricular remodeling and dysfunction after experimental myocardial infarction: a new action for an old drug? *Circulation* 110: 2175–2179, 2004.
13. Epstein FH, Yang Z, Gilson WD, Berr SS, Kramer CM, and French BA. MR Tagging early after myocardial infarction in mice demonstrates contractile dysfunction in adjacent and remote regions. *Magn Reson Med* 48: 399–403, 2002.
14. Epstein FH, Yang Z, Roy RJ, Xu Y, Berr SS, and French BA. CMR demonstrates reduced post-infarct left ventricular remodeling in mice with iNOS inhibition. *J Cardiovasc Magn Res* 7: 29–30, 2005.
15. Hardy CJ, Weiss RG, Bottomley PA, and Gerstenblith G. Altered myocardial high-energy phosphate metabolites in patients with dilated cardiomyopathy. *Am Heart J* 122: 795–801, 1991.
16. Horn M, Remkes H, Strömer H, Dienesch C, and Neubauer S. Chronic phosphocreatine depletion by the creatine analogue β -guanidinopropionate is associated with increased mortality and loss of ATP in rats after myocardial infarction. *Circulation* 104: 1844–1849, 2001.
17. Hügel S, Horn M, Groot M, and Remkes H. Effects of ACE inhibition and β -receptor blockade on energy metabolism in rats postmyocardial infarction. *Am J Physiol Heart Circ Physiol* 277: H2167–H2175, 1999.
18. Hügel S, Horn M, Remkes H, Dienesch C, and Neubauer S. Preservation of cardiac function and energy reserve by the angiotensin-converting enzyme inhibitor quinapril during postmyocardial infarction remodeling in the rat. *J Cardiovasc Magn Reson* 3: 215–225, 2001.



19. Illing B, Horn M, Urban B, Stromer H, Schnackerz K, de Groot M, Haase A, Hu K, Ertl G, and Neubauer S. Changes of myocardial high-energy phosphates with the cardiac cycle during acute or chronic myocardial stress. *Magn Reson Med* 40: 727–732, 1998.

20. Ingwall JS. Phosphorus nuclear magnetic resonance spectroscopy of cardiac and skeletal muscles. *Am J Physiol Heart Circ Physiol* 242: H729–H744, 1982.

21. Ingwall JS and Weiss RG. Is the failing heart energy starved? On using chemical energy to support cardiac function. *Circ Res* 95: 135–145, 2004.

22. Katz AM. Is the failing heart energy depleted? *Cardiol Clin* 16: 633–644, 1998.

23. Laser A, Ingwall JS, Tian R, Reis I, Hu K, Gaudron P, Ertl G, and Neubauer S. Regional biochemical remodeling in non-infarcted tissue of rat heart post-myocardial infarction. *J Mol Cell Cardiol* 28: 1531–1538, 1996.

24. Liao R, Jain M, Cui L, D’Agostino J, Aiello F, Luptak I, Ngoy S, Mortensen RM, and Tian R. Cardiac-specific overexpression of GLUT1 prevents the development of heart failure attributable to pressure overload in mice. *Circulation* 106: 2125–2131, 2002.

25. Lutgens E, Daemen MJ, de Muinck ED, Debets J, Leenders P, and Smits JF. Chronic myocardial infarction in the mouse: cardiac structural and functional changes. *Cardiovasc Res* 41: 586–593, 1999.

26. Menon RS, Hendrich K, Hu X, and Ugurbil K. ³¹P NMR spectroscopy of the human heart at 4T: detection of substantially uncontaminated cardiac spectra and differentiation of subepicardium and subendocardium. *Magn Reson Med* 26: 368–376, 1992.

27. Mitchell GF and Pfeffer MA. Left ventricular remodeling after myocardial infarction: progression toward heart failure. *Heart Failure* 8: 55–69, 1999.

28. Murakami Y, Zhang Y, Cho YK, Mansoor AM, Chung JK, Chu C, Francis G, Ugurbil K, Bache RJ, From AH, Jerosch-Herold M, Wilke N, and Zhang J. Myocardial oxygenation during high work states in hearts with postinfarction remodeling. *Circulation* 99: 942–948, 1999.

29. Murakami Y, Zhang J, Eijgelshoven MHJ, Chen W, Carlyle WC, Zhang Y, Gong G, and Bache RJ. Myocardial creatine kinase kinetics in hearts with postinfarction left ventricular remodeling. *Am J Physiol Heart Circ Physiol* 276: H892–H900, 1999.

30. Nahrendorf M, Hiller KH, Hu K, Ertl G, Haase A, and Bauer WR. Cardiac magnetic resonance imaging in small animal models of human heart failure. *Med Image Anal* 7: 369–375, 2003.

31. Neubauer S, Horn M, Cramer M, Harre K, Newell JB, Peters W, Pabst T, Ertl G, Hahn D, Ingwall JS, and Kochsiek K. Myocardial phosphocreatine-to-ATP ratio is a predictor of mortality in patients with dilated cardiomyopathy. *Circulation* 96: 2190–2196, 1997.

32. Neubauer S, Horn M, Naumann A, Tian R, Hu K, Laser M, Friedrich J, Gaudron P, Schnackerz K, Ingwall JS, and Ertl G. Impairment of energy metabolism in intact residual myocardium of rat hearts with chronic myocardial infarction. *J Clin Invest* 95: 1092–1100, 1995.

33. Neubauer S, Hu K, Horn M, Remkes H, Hoffmann KD, Schmidt C, Schmidt TJ, Schnackerz K, and Ertl G. Functional and energetic consequences of chronic myocardial creatine depletion by β-guanidino-propionate in perfused hearts and in intact rats. *J Mol Cell Cardiol* 31: 1845–1855, 1999.

34. Neubauer S, Krahe T, Schindler R, Horn M, Hillenbrand H, Entzeroth C, Mader H, Kromer EP, Riegger GAJ, Lackner K, and Ertl G. ³¹P Magnetic resonance spectroscopy in dilated cardiomyopathy and coronary artery disease: altered ventricular high-energy phosphate metabolism in heart failure. *Circulation* 86: 1810–1818, 1992.

35. Neubauer S, Remkes H, Spindler M, Horn M, Wiesmann F, Prestle J, Walzel B, Ertl G, Hasenfuss G, and Wallimann T. Downregulation of the Na⁺-creatinine cotransporter in failing human myocardium and in experimental heart failure. *Circulation* 100: 1847–1850, 1999.

36. Olivetti G, Capasso JM, Meggs LG, Sonnenblick EH, and Anversa P. Cellular basis of chronic ventricular remodeling after myocardial infarction in rats. *Circ Res* 68: 856–869, 1991.

37. Omerovic E, Bollano E, Basetti M, Kujacic V, Waagstein L, Hjalmarsson A, Waagstein F, and Soussi B. Bioenergetic, functional and morphological consequences of postinfarct cardiac remodeling in the rat. *J Mol Cell Cardiol* 31: 1685–1695, 1999.

38. Patten RD, Aronovitz MJ, Deras-Mejia L, Pandian NG, Hanak GG, Smith JJ, Mendelsohn ME, and Konstam MA. Ventricular remodeling in a mouse model of myocardial infarction. *Am J Physiol Heart Circ Physiol* 274: H1812–H1820, 1998.

39. Pérez NG, Gao WD, and Marbán E. Novel myofilament CA²⁺-sensitizing property of xanthine oxidase inhibitors. *Circ Res* 83: 423–430, 1998.

40. Pfeffer MA. Enhancing cardiac protection after myocardial infarction: rationale for newer clinical trials of angiotensin receptor blockers. *Am Heart J* 139: S23–S28, 2000.

41. Pfeffer MA, McMurray JJV, Velazquez EJ, Rouleau JL, Køber L, Maggioni AP, Solomon SD, Swedberg K, Werf FV, White H, Leimberger JD, Henis M, Edwards S, Zelenkofske S, Sellers MA, and Califf RM. Valsartan, captopril, or both in myocardial infarction complicated by heart failure, left ventricular dysfunction, or both. *N Engl J Med* 349: 1893–1906, 2003.

42. Shen W, Asai K, Uechi M, Mathier MA, Shannon RP, Vatner SF, and Ingwall JS. Progressive loss of myocardial ATP due to a loss of total purines during the development of heart failure in dogs: a compensatory role for the parallel loss of creatine. *Circulation* 100: 2113–2118, 1999.

43. Stull LB, Leppo MK, Gao WD, and Marbán E. Chronic treatment with allopurinol boosts survival and cardiac contractility in murine postischemic cardiomyopathy. *Circ Res* 95: 1005–1011, 2004.

44. Udelson JE, Patten RD, and Konstam MA. New concepts in post-infarction ventricular remodeling. *Rev Cardiovasc Med* 4: S3–S12, 2003.

45. Von Kienlin M, Rosch C, Le Fur Y, Behr W, Roder F, Haase A, Horn M, Illing B, Hu K, Ertl G, and Neubauer S. Three-dimensional ³¹P magnetic resonance spectroscopic imaging of regional high-energy phosphate metabolism in injured rat heart. *Magn Reson Med* 39: 731–741, 1998.

46. Weiss RG, Bottomley PA, Hardy CJ, and Gerstenblith G. Regional myocardial metabolism of high-energy phosphates during isometric exercise in patients with coronary artery disease. *N Engl J Med* 323: 1593–1600, 1990.

47. Weiss RG, Chatham JC, Georgakopoulos D, Wallimann T, Kay L, Walzel B, Wang Y, Kass DA, Gerstenblith G, and Chacko VP. An increase in the myocardial PCr/ATP ratio in GLUT4 null mice. *FASEB J* 16: 613–615, 2002.

48. Weiss RG, Kalil-Filho R, Herskowitz A, Chacko VP, Stern MD, and Gerstenblith G. Tricarboxylic acid cycle activity in post-ischemic rat hearts. *Circulation* 87: 270–282, 1993.

49. Yabe T, Mitsunami K, Inubushi T, and Kinoshita M. Quantitative measurements of cardiac phosphorus metabolites in coronary artery disease by ³¹P magnetic resonance spectroscopy. *Circulation* 92: 15–23, 1995.

50. Yang Z, Berr SS, Gilson WD, Toufektsian M, and French BA. Simultaneous evaluation of infarct size and cardiac function in intact mice by contrast-enhanced cardiac magnetic resonance imaging reveals contractile dysfunction in noninfarcted regions early after myocardial infarction. *Circulation* 109: 1161–1167, 2004.

Downloaded from ajpheart.physiology.org on September 7, 2006